

Mieite-(Y), $Y_4Ti(SiO_4)_2O[F,(OH)]_6$, a new mineral in a pegmatite at Souri Valley, Komono, Mie Prefecture, central Japan

Ritsuro MIYAWAKI*, Satoshi MATSUBARA*, Kazumi YOKOYAMA*, Masako SHIGEOKA*,
Koichi MOMMA* and Sadaoki YAMAMOTO**

*Department of Geology and Paleontology, National Museum of Nature and Science,
4-1-1 Amakubo, Tsukuba, Ibaraki 305-0005, Japan

**Obiracho, Yokkaichi, Mie 512-0921, Japan

Mieite-(Y), ideally $Y_4Ti(SiO_4)_2O[F,(OH)]_6$, was found in a pegmatite at Souri Valley, Komono, Mie Prefecture, central Japan. It occurs as an amber yellow mass with adamantine luster, approximate size of 1 cm and white streak. The mineral is associated with quartz, albite, K-feldspar, muscovite, allanite-(Ce), gadolinite-(Y), and magnesianrowlandite-(Y). Cleavage is not observed and fracture is uneven. The Mohs hardness is 6. The calculated density is 4.61 g/cm³. It is biaxial and refractive indices are $\alpha = 1.694(2)$ and $\gamma = 1.715(5)$ with non-pleochroism. The mineral displays anomalous blue interference colors. The empirical formula is $(Y_{3.13}Dy_{0.20}Gd_{0.17}Yb_{0.08}Nd_{0.08}Sm_{0.07}Er_{0.07}Th_{0.05}Tb_{0.03}Ho_{0.03}Lu_{0.03}Ce_{0.02}Tm_{0.02}U_{0.02})_{\Sigma 4.00}(Ti_{0.52}Al_{0.44}Fe_{0.01})_{\Sigma 0.97}(Si_{1.92}P_{0.12})_{\Sigma 2.04}O_9[F_{3.83}(OH)_{1.91}]_{\Sigma 5.74}$ on the basis of 7 cations and 9 oxygen atoms *pfu* after electron microprobe (WDS), FT/IR and crystal structure analyses by means of single crystal XRD data. The raw material is significantly metamictized to give extremely weak diffraction peaks. The unit cell parameters refined from powder XRD pattern of recrystallized material are; $a = 14.979(6)$, $b = 10.548(5)$, $c = 6.964(3)$ Å, $V = 1100.3(8)$ Å³ and $Z = 4$. The 7 strongest lines in the powder XRD pattern [$d(\text{Å})$ (I/I_0) hkl] are; 2.68 (100) 331, 3.76 (85) 400, 3.54 (83) 002, 3.48 (82) 130, 2.16 (78) 023, 4.26 (68) 021, 5.46 (58) 111. The crystal structure was refined in space group *Cmcm* to $R_1 = 0.0825$ and 0.0735 for 491 and 581 reflections with $I > 2\sigma(I)$ single crystal XRD data of raw and recrystallized materials, respectively. The crystal structure of mieite-(Y) consists of infinite columns of corner-sharing TiO_6 octahedra decorated by SiO_4 tetrahedra. The columns are linked by two independent Y polyhedra with different coordination, YO_2F_5 and YO_5F_3 . A coupled substitution of $Ti^{4+} + F^- = Al^{3+} + \square$ (vacancy) was suggested for mieite-(Y). Mieite-(Y) is isostructural with the ‘yftisite’, a discredited species. Mieite-(Y) can be classified in the Dana class 52.4.4.3 and Strunz class 9.AG.25, nesosilicates with additional anions.

Keywords: Mieite-(Y), Yftisite, New mineral, Souri Valley, Mie

INTRODUCTION

A fluoride silicate of rare earth elements (REEs), of which Y is the predominant, and Ti was recognized, following magnesianrowlandite-(Y) (Matsubara et al., 2014), among unfamiliar minerals showing appearance similar to fluorthalénite-(Y) collected by the last author (S.Y.) from a pegmatite at Souri Valley, in Komono, Mie Prefecture, central Japan. The chemical and X-ray diffraction studies indicated that it is identical with ‘yftisite’ from Kola Peninsula, Russia (Pletneva, et al., 1971; Ballo and Bakakin, 1975). No information has been given in

any literatures on the type specimen of ‘yftisite’, and on the approval as a new species by the IMA Commission on New Minerals and Mineral Names, CNMNMN, which was merged with the Commission on Classification of Minerals into the Commission on New Minerals, Nomenclature and Classification (CNMNC) in July of 2006. Fleischer and Jambor (1977) recommended that the mineral should not have been named until better chemical data were available, although the mineral was an independent species. The CNMNMN discredited ‘yftisite’ due to its incomplete chemical analysis (Nickel and Mandarino, 1987). ‘Yftisite’ is not a valid mineral species. Consequently, there is no valid type specimen of ‘yftisite’ to be re-examined for the re-definition and comparison.

The authors agree with the suggestion of the Chair-

man of CNMNC to have a new name instead of re-using the name of a comparatively recently discredited mineral. The fluoride silicate mineral of REEs and Ti from Souri Valley is named as mieite-(Y) after the locality, Mie (pronounced as mi-e; 'mi' for mineral and 'e' for essential) Prefecture. The mineral data and the name have been approved by the IMA-CNMC (no. 2014-020). The type specimen is deposited at the National Museum of Nature and Science, Japan, under the registered number NSM-M43627.

OCCURRENCE

Mieite-(Y) was recognized in specimens from the pegmatite block, where magnesiorowlandite-(Y) was found (Matsubara et al., 2014), in Souri Valley located in Komono, Mie Prefecture, central Japan (35°0'35"N, 136°27'33"E). The pegmatite is a part of the Cretaceous Suzuka granite (Harayama et al., 1989). Mieite-(Y) occurs in the pegmatite composed of quartz, albite, K-feldspar and muscovite in association with accessory minerals of REEs, such as allanite-(Ce), gadolinite-(Y) and magnesiorowlandite-(Y). Mieite-(Y) forms an amber yellow mass with adamantine luster (Fig. 1). The aggregate is about 1 cm in diameter. The appearance is similar to that of fluorthalénite-(Y).



Figure 1. Photograph of the type specimen of mieite-(Y) in a pegmatite. The position of mieite-(Y) is indicated by a red arrow.

PHYSICAL AND OPTICAL PROPERTIES

The cleavage is not observed and fracture is uneven. The tenacity is brittle. The density could not be measured directly, but the calculated density is 4.61 g/cm³ on the basis of the empirical formula and refined unit cell dimensions. The hardness is 6 on the Mohs scale. Mieite-(Y) is pale amber yellow with white streak. It is transparent with adamantine luster. The mineral is biaxial and refractive indices are $\alpha = 1.694(2)$ and $\gamma = 1.715(5)$ with non-pleochroism. The mineral displays anomalous blue interference colors.

CHEMICAL COMPOSITION

Chemical analysis was carried out with a JEOL JXA-8800M WDS electron microprobe analyzer (15 kV, 1 nA, beam diameter 3 μ m). The FT/IR (JASCO FT/IR-420) spectrum (Fig. 2) exhibits an absorption band at 3400 cm⁻¹ due to O-H stretching, and broad bands from 900 to 1100 cm⁻¹ due to Si-O, Ti-O and Al-O bonds. A weak absorption at 1650 cm⁻¹ (H-O-H bending) may be due to the water absorbed on the KBr pellet. This suggests that the band at 3400 cm⁻¹ is principally due to the OH⁻ anion substituting for F⁻ in the crystal lattice. The concentration of H₂O corresponding to the OH⁻ anions was calculated by the difference between the determined F concentration and the stoichiometry from the results of the crystal structure analysis. The averaged values for 7 analyses and standard materials are shown in Table 1. The empirical formula is (Y_{3.13}Dy_{0.20}Gd_{0.17}Yb_{0.08}Nd_{0.08}Sm_{0.07}Er_{0.07}Th_{0.05}Tb_{0.03}Ho_{0.03}Lu_{0.03}Ce_{0.02}Tm_{0.02}U_{0.02}) Σ 4.00 (Ti_{0.52}Al_{0.44}Fe_{0.01}) Σ 0.97(Si_{1.92}P_{0.12}) Σ 2.04O₉[F_{3.83}(OH)_{1.91}] Σ 5.74 on the basis of 7 cations and 9 oxygen atoms *pfu*. The simplified and ideal formulae are (Y,Dy,Th)₄(Ti,Al)[(Si,P)O₄]₂O[F,(OH),□]₆ and Y₄Ti(SiO₄)₂OF₆, respectively.

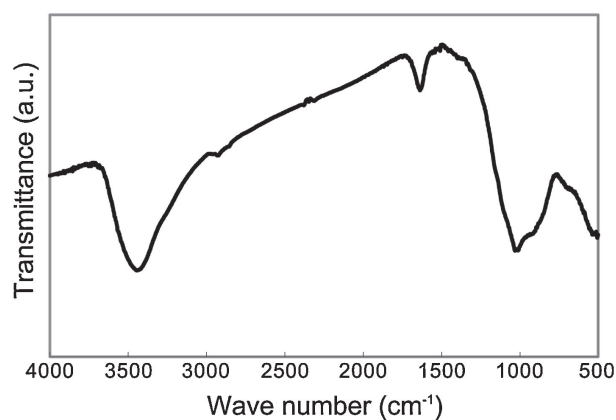


Figure 2. Infrared absorption spectrum of mieite-(Y).

Table 1. Chemical composition of mieite-(Y)

Constituent	wt%	Range	SD	Probe standard
SiO ₂	14.70	14.60 – 14.79	0.06	Fayalite
P ₂ O ₅	1.06	0.95 – 1.10	0.05	DyP ₅ O ₁₄
TiO ₂	5.32	5.14 – 5.57	0.15	Anatase
Al ₂ O ₃	2.84	2.66 – 2.94	0.09	Sillimanite
Fe ₂ O ₃	0.06	0.04 – 0.09	0.01	Fayalite
Y ₂ O ₃	45.14	44.04 – 45.83	0.56	YP ₅ O ₁₄
La ₂ O ₃	n.d			LaP ₅ O ₁₄
Ce ₂ O ₃	0.39	0.26 – 0.56	0.10	CeP ₅ O ₁₄
Pr ₂ O ₃	0.10	0.00 – 0.49	0.16	PrP ₅ O ₁₄
Nd ₂ O ₃	1.62	1.51 – 1.68	0.05	NdP ₅ O ₁₄
Sm ₂ O ₃	1.59	1.15 – 1.79	0.13	SmP ₅ O ₁₄
Gd ₂ O ₃	3.99	3.76 – 4.11	0.11	GdP ₅ O ₁₄
Tb ₂ O ₃	0.73	0.50 – 0.85	0.12	TbP ₅ O ₁₄
Dy ₂ O ₃	4.70	4.22 – 4.93	0.21	DyP ₅ O ₁₄
Ho ₂ O ₃	0.65	0.52 – 0.77	0.08	HoP ₅ O ₁₄
Er ₂ O ₃	1.73	1.55 – 1.94	0.15	ErP ₅ O ₁₄
Tm ₂ O ₃	0.39	0.21 – 0.62	0.14	TmP ₅ O ₁₄
Yb ₂ O ₃	2.13	2.01 – 2.25	0.09	YbP ₅ O ₁₄
Lu ₂ O ₃	0.77	0.54 – 0.95	0.13	LuP ₅ O ₁₄
ThO ₂	1.59	0.07 – 0.49	0.11	ThO ₂
UO ₂	0.63	0.55 – 0.68	0.04	UO ₂
F	9.28	8.89 – 9.63	0.28	CaF ₂
H ₂ O	2.19			Calculated
O = F	-3.91			
Total	97.69			

X-RAY CRYSTALLOGRAPHY

X-ray diffraction investigations were carried out with the raw and annealed materials. X-ray diffraction data were examined for raw and annealed materials. The raw material is significantly metamictized to give extremely weak diffraction peaks (Fig. 3). Some trials to recover the original crystal structure were carried out with several fragments (less than 1 mg) per a run in a Pt cup on a RIGAKU Thermo plus 2 / TG-8120 thermal analyzer. The annealing at 810 °C made X-ray diffraction peaks intense and clear, whereas samples treated under 800 °C showed diffraction patterns as poor as the raw material. The X-ray diffraction pattern of the sample annealed at 900 °C is different from the others to show a phase transition into an unidentified phase giving a broad diffraction pattern which could not be assigned to any known phases (Fig. 3).

X-ray diffraction data were examined for the raw and recrystallized (annealed at 810 °C) materials. The powder X-ray diffraction patterns were obtained using a Gandolfi camera, 114.6 mm in diameter, employing Ni-filtered CuK α radiation. The data were recorded on an imaging plate (IP), and were processed with a Fuji BAS-2500 bio-image analyzer using a computer program written by Nakamura (1999). The X-ray diffraction patterns (Table 2) are basically identical with those of

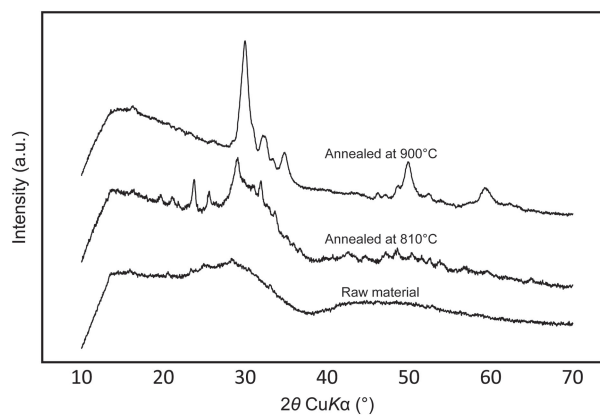


Figure 3. Powder X-ray diffraction patterns of the raw and recrystallized mieite-(Y). The pattern of sample annealed at 810 °C is given as representative data for recrystallized materials. The pattern of unidentified phase transitioned by means of annealing at 900 °C from the metamictized mieite-(Y) is also given for comparison.

annealed sample of ‘yftisite’ from Kola Peninsula, Russia (Pletneva et al., 1971). The reflections of powder X-ray diffraction pattern were indexed by reference to the single crystal X-ray diffraction data. The unit cell parameters of the orthorhombic system were refined with an internal Si-standard reference material (NBS #640b) using a computer program by Toraya (1993); $a = 15.03(3)$, $b = 10.67(1)$, $c = 7.071(8)$ Å, $V = 1133(3)$ Å³ and $Z = 4$ (raw material), and $a = 14.979(6)$, $b = 10.548(5)$, $c = 6.964(3)$ Å, $V = 1100.3(8)$ Å³ and $Z = 4$ (recrystallized material). These values are comparable to those refined from the single crystal X-ray diffraction data (Tables 2 and 3).

The single crystal X-ray diffraction data were collected on a Rigaku R-AXIS RAPID curved imaging plate diffractometer using MoK α radiation monochromated and focused by a VariMax confocal multilayer mirror. Experimental details of the data collection procedure are given in Table 3. The data were empirically corrected for absorption, Lorentz and polarization effects. The crystal structure was analyzed using the direct method with the Patterson calculation by means of SHELXS-97 (Sheldrick, 2008) for the raw material, i.e., partially metamictized crystal without the annealing for recrystallization. The positions of Y, Ti, Si, and some O and F atoms were determined to be identical with those in the result of the crystal structure analysis of ‘yftisite’ by Balko and Bakakin (1975). Full-matrix least-square refinement was carried out with SHELXL-97 (Sheldrick, 2008), employing the scattering factors for the neutral atoms and anomalous dispersion factors were taken from the International Tables for X-ray Crystallography, Volume C (1992). The scattering curve of Dy was employed in the calculations

Table 2. Powder X-ray diffraction data for mieite-(Y) and 'yftsite'

	Mieite-(Y), raw material Souri*						Mieite-(Y), annealed at 810 °C Souri*						'Yftsite' Kola Peninsula**	
	Powder data			Single crystal data			Powder data			Single crystal data			Powder data	
	<i>h k l</i>	<i>I/I₀</i>	<i>d_{obs.}</i>	<i>d_{calc.}</i>	<i>I_{calc.}</i>	<i>d_{calc.}</i>	<i>I/I₀</i>	<i>d_{obs.}</i>	<i>d_{calc.}</i>	<i>I_{calc.}</i>	<i>d_{calc.}</i>	<i>I</i>	<i>d</i>	
<i>a</i> (Å)	15.03(3)			14.9424(19)			14.979(6)			14.934(13)			15.04(1)	
<i>b</i> (Å)	10.668(11)			10.6332(15)			10.548(5)			10.530(9)			10.63(1)	
<i>c</i> (Å)	7.071(8)			7.0365(8)			6.964(3)			6.952(6)			7.052(3)	
<i>V</i> (Å ³)	1133(3)			1118.0(3)			1100.3(8)			1093.2(16)			1127	
1 1 1	58	5.46	5.49	19	5.46	13	5.40	5.42	19	5.41				
3 1 0			4.53	37	4.51	12	4.51	4.51	31	4.50		20	4.49	
0 2 1	68	4.26	4.26	45	4.24	18	4.20	4.20	46	4.20		20	4.25	
						10	4.06							
4 0 0	85	3.76	3.76	98	3.74	56	3.74	3.74	100	3.73				
2 2 1			3.70	0	3.69				0	3.66		70	3.727	
0 0 2	83	3.54	3.54	100	3.52	31	3.48	3.48	95	3.48		70	3.526	
1 3 0	82	3.48	3.46	13	3.45				13	3.42		10	3.353	
						13	3.38							
1 1 2			3.28	14	3.26			3.23	13	3.22		10	3.265	
2 0 2			3.20	18	3.18			3.16	20	3.15				
1 3 1			3.11	79	3.10	100	3.07	3.07	71	3.07		100	3.099	
3 3 0			2.90			66	2.88	2.87	32	2.87		50	2.891	
4 2 1			2.82	32	2.89	81	2.80	2.80	18	2.79		20	2.817	
						51	2.73							
3 3 1	100	2.68	2.68	72	2.67	45	2.66	2.66	67	2.65				
5 1 1			2.68	12	2.66			2.66	10	2.66				
0 4 0				0	2.66				1	2.63		100	2.667	
4 0 2			2.57	34	2.56	16	2.55	2.55	34	2.54		50	2.566	
6 0 0			2.50	15	2.49	10	2.49	2.50	15	2.49		40b	2.499	
1 3 2	54	2.43	2.47	22	2.46	8	2.44	2.44	25	2.44		40b	2.463	
5 3 0			2.30	14	2.28	10	2.26	2.28	11	2.27		30	2.287	
3 3 2	37	2.23	2.24	23	2.23	9	2.22	2.22	23	2.21				
5 1 2			2.24	0	2.23				0	2.21		30	2.237	
0 2 3	78	2.16	2.16	32	2.15	16	2.12	2.12	32	2.12		60	2.153	
1 5 0	54	2.11	2.11	11	2.11			2.09	11	2.09				
7 1 0			2.10	5	2.09				6	2.09		20	2.102	
6 0 2	48	2.07	2.04	11	2.03	9	2.03	2.03	14	2.02				
1 3 3			1.948	21	1.939			1.921	19	1.918		60b	1.949	
8 0 0			1.878	11	1.868	16	1.874	1.872	13	1.867				
4 2 3			1.870	21	1.861			1.848	24	1.844		40	1.865	
3 3 3			1.829	33	1.821	9	1.811	1.806	31	1.803				
6 4 0			1.826	0	1.817				0	1.809		90	1.821	
7 3 1			1.779	29	1.770	9	1.766	1.768	30	1.763				
6 4 1			1.768	3	1.760				3	1.750		100	1.766	
0 0 4			1.768	26	1.759	9	1.741	1.741	25	1.738				
0 6 1	46	1.717	1.724	23	1.719			1.705	23	1.702				
3 5 2			1.716	11	1.709	10	1.698	1.697	12	1.694		100	1.714	
7 3 2			1.631	17	1.623	14	1.618	1.618	21	1.615				
6 4 2			1.622	2	1.615				3	1.604		40	1.622	
1 3 4			1.574	2	1.567				3	1.549		10b	1.573	
4 6 1			1.567	25	1.561	9	1.551	1.551	23	1.548				
5 5 2			1.561	4	1.554				4	1.542		80	1.559	
3 3 4				10	1.502									
100 0			1.503	1	1.494							50	1.504	
7 3 3	47	1.431	1.449	21	1.442							80	1.442	
6 4 3			1.443	2	1.437									

* Souri Valley, central Japan. Present study.

** Kola Peninsula, Russia. ICDD 33-1462. (Pletneva et al., 1971).

to represent the lanthanoids (Ln; La-Lu). That of F was simply used for the F sites, but the substitution of (OH) for F was not examined in the refinements. The occupancy parameters were fixed to 0.77Y + 0.23Dy and 0.55Ti + 0.45Al for the Y and Ti sites, respectively, in the later

cycles of refinements according to the chemical composition. The refinement with the full occupancy of F at the F sites converged into $R_1 = 0.0816$ for 491 observed reflections with the criteria of $I > 2\sigma(I)$. To neutralize the unbalanced structural formula calculated from the occu-

Table 3. Crystal data, data collection information, and refinement details

	Raw material	Annealed at 810 °C
Space group	<i>Cmcm</i> (# 63)	
Cell parameters		
<i>a</i> (Å)	14.9424(19)	14.934(13)
<i>b</i> (Å)	10.6332(15)	10.530(9)
<i>c</i> (Å)	7.0365(8)	6.952(6)
<i>V</i> (Å ³)	1118.0(3)	1093.2(16)
<i>Z</i>	4	4
Structural formula	(Y _{3.08} Dy _{0.92})(Ti _{0.55} Al _{0.45})(SiO ₄) ₂ O[F,(OH)] _{5.55}	
<i>D</i> _{calc.} (g/cm ³)	4.602	4.706
μ (mm ⁻¹)	22.63	23.14
Data collection		
Temperature (K)	293	293
Crystal size (mm)	0.2 × 0.1 × 0.05	0.05 × 0.05 × 0.02
Diffractometer	Rigaku VariMax/R-axis RAPID	
Radiation	MoK α (monochromated and focused by a confocal multilayer mirror)	
Readout pixel mode (mm)	0.100	0.100
2 θ range (°)	6 – 55	6 – 55
Total oscillation images	44	220
First sweep ω (°)	130.0 – 190.0 in 5.0 step	130.0 – 190.0 in 1.0 step
χ (°)	45.0	45.0
φ (°)	0.0	0.0
exposure rate (s ^o)	300	120
Second sweep ω (°)	0.0 – 160.0 in 5.0 step	0.0 – 160.0 in 1.0 step
χ (°)	45.0	45.0
φ (°)	180.0	180.0
exposure rate (s ^o)	300	120
Index ranges	-18 ≤ <i>h</i> ≤ 19; -13 ≤ <i>k</i> ≤ 13; -9 ≤ <i>l</i> ≤ 8	-18 ≤ <i>h</i> ≤ 19; -13 ≤ <i>k</i> ≤ 13; -9 ≤ <i>l</i> ≤ 8
No. measured reflections	5217	5104
No. unique reflections	713	702
No. reflections, <i>I</i> > 2 σ (<i>I</i>)	491	581
<i>R</i> _{int.}	0.1441	0.1015
Refinement		
No. parameters	65	65
<i>R</i> ₁ , <i>I</i> > 2 σ (<i>I</i>)	0.0825	0.0735
<i>R</i> ₁ , all data	0.1127	0.0867
<i>wR</i> ₂ , all data	0.2592	0.2456
Weighting parameters; <i>a</i> , <i>b</i>	0.1, 0	0.1, 0
GOF	1.502	1.759
$\Delta\rho_{\min}$, $\Delta\rho_{\max}$ (e / Å ³)	-2.646, 2.921	-2.384, 3.345

$$R_1 = \frac{\sum ||F_o| - |F_c||}{\sum |F_o|}$$

$$wR_2 = \left\{ \frac{\sum [w(F_o^2 - F_c^2)^2]}{\sum [w(F_o^2)]} \right\}^{0.5}$$

$$w = 1 / [\sigma^2(F_o^2) + (aP)^2 + bP]$$

$$P = [2 F_c^2 + F_o^2] / 3$$

pancy parameters, (Y_{0.77}Dy_{0.23})₄(Ti_{0.55}Al_{0.45})(SiO)₂OF₆, a vacancy was introduced into the F3 site in the final cycles of refinement for the raw material, following the refinement of the recrystallized material as described below. The occupancy parameters of Ti and F3 were equivalently kept to be 0.55, corresponding to the neutralized structural formula; (Y_{0.77}Dy_{0.23})₄(Ti_{0.55}Al_{0.45})(SiO)₂OF_{5.55} (Table 4).

The refinement for the recrystallized fragment indicated that partial vacancy at the F3 site, the occupancy parameter of 0.40(7) with *R*₁ = 0.0738 for 581 observed

reflections with the criteria of *I* > 2 σ (*I*). It suggests a coupled substitution of Ti⁴⁺ + F⁻ = Al³⁺ + □ (vacancy) as a charge compensating mechanism in the crystal structure of mieite-(Y). In accordance with the substitution, the occupancy parameter of F3 was fixed to be 0.55, the same to that of Ti against Al in the Ti site, in the final cycles of refinement for the recrystallized material.

The final positional parameters and anisotropic displacement parameters with equivalent isotropic displacement parameters of raw and recrystallized materials are given in Tables 4 and 5, respectively. Selected inter-

Table 4. Final atom positions and anisotropic displacement parameters (\AA^2) with equivalent isotropic displacement parameters for mieite-(Y) without annealing

Atom	x/a	y/b	z/c	U_{eq}	U_{11}	U_{22}	U_{33}	U_{23}	U_{13}	U_{12}
Y1*	0.14448(16)	0.4359(2)	0.25	0.0411(8)	0.0409(15)	0.0395(16)	0.0429(14)	0.0	0.0	-0.0023(11)
Y2*	0.13098(14)	0.79425(19)	0.25	0.0303(7)	0.0301(12)	0.0208(11)	0.0401(13)	0.0	0.0	0.0031(8)
Ti**	0.0	0.0	0.5	0.0249(17)	0.024(4)	0.020(4)	0.031(4)	-0.005(3)	0.0	0.0
Si	0.1549(6)	0.1201(7)	0.25	0.0344(18)	0.035(4)	0.031(5)	0.037(4)	0.0	0.0	0.002(3)
O1	0.0927(9)	0.1285(11)	0.0555(19)	0.033(3)	0.031(7)	0.032(8)	0.037(7)	-0.001(5)	-0.009(6)	0.000(6)
O2	0.2903(12)	0.488(2)	0.25	0.041(5)	0.022(10)	0.049(13)	0.052(12)	0.0	0.0	0.010(9)
O3	0.2175(12)	0.2485(19)	0.25	0.038(5)	0.026(10)	0.022(10)	0.065(13)	0.0	0.0	0.007(8)
O4	0.5	0.438(3)	0.25	0.034(6)	0.010(11)	0.058(19)	0.034(15)	0.0	0.0	0.0
F1	0.3591(9)	0.1149(11)	0.0605(18)	0.050(4)	0.077(10)	0.038(8)	0.037(6)	-0.006(5)	0.007(6)	-0.011(6)
F2	0.0	0.395(5)	0.25	0.122(19)	0.028(16)	0.28(6)	0.06(2)	0.0	0.0	0.0
F3***	0.0	0.699(3)	0.25	0.023(7)	0.009(15)	0.03(2)	0.034(19)	0.0	0.0	0.0

* 0.77Y + 0.23Dy. ** 0.55Ti + 0.45Al. *** 0.55F.

Table 5. Final atom positions and anisotropic displacement parameters (\AA^2) with equivalent isotropic displacement parameters for mieite-(Y) annealed at 810 °C

Atom	x/a	y/b	z/c	U_{eq}	U_{11}	U_{22}	U_{33}	U_{23}	U_{13}	U_{12}
Y1*	0.14461(11)	0.43548(18)	0.25	0.0258(7)	0.0254(10)	0.0258(12)	0.0262(10)	0.0	0.0	-0.0003(6)
Y2*	0.13266(11)	0.79844(16)	0.25	0.0217(6)	0.0201(10)	0.0229(10)	0.0222(10)	0.0	0.0	0.0020(6)
Ti**	0.0	0.0	0.5	0.0139(12)	0.016(3)	0.013(3)	0.013(2)	-0.0007(19)	0.0	0.0
Si	0.1553(4)	0.1194(5)	0.25	0.0188(13)	0.020(3)	0.019(3)	0.018(3)	0.0	0.0	-0.0027(19)
O1	0.0927(7)	0.1244(9)	0.0562(14)	0.019(2)	0.019(4)	0.020(5)	0.019(5)	-0.001(3)	0.001(4)	0.002(3)
O2	0.2875(8)	0.4881(13)	0.25	0.019(3)	0.008(6)	0.011(7)	0.039(7)	0.0	0.0	0.002(5)
O3	0.2164(10)	0.2467(15)	0.25	0.026(3)	0.031(8)	0.018(7)	0.031(7)	0.0	0.0	-0.004(6)
O4	0.5	0.435(2)	0.25	0.027(5)	0.022(10)	0.039(14)	0.021(9)	0.0	0.0	0.0
F1	0.3647(7)	0.1156(8)	0.0627(15)	0.035(3)	0.051(6)	0.024(6)	0.029(5)	-0.002(3)	0.006(5)	-0.001(4)
F2	0.0	0.417(3)	0.25	0.082(10)	0.025(11)	0.053(17)	0.17(3)	0.0	0.0	0.0
F3***	0.0	0.689(5)	0.25	0.054(11)	0.023(19)	0.06(3)	0.08(3)	0.0	0.0	0.0

* 0.77Y + 0.23Dy. ** 0.55Ti + 0.45Al. *** 0.55F.

Table 6. Interatomic distances (\AA) for mieite-(Y)

		Raw material	Annealed			Raw material	Annealed
Y1	— F2	2.203(10)	2.169(4)	Y2	— F3	2.203(16)	2.29(2)
	— F1	2.251(12) × 2	2.244(10) × 2		— O3	2.315(18)	2.318(15)
	— O2	2.249(19)	2.205(12)		— F1	2.331(11) × 2	2.324(9) × 2
	— O3	2.271(19)	2.258(16)		— O1	2.371(14) × 2	2.355(10) × 2
	— F1	2.325(12) × 2	2.305(9) × 2		— O2	2.37(2)	2.326(13)
Mean	2.268	2.247	— O4	2.483(18)	2.451(14)		
Si	— O2	1.63(2)	1.624(14)	Mean	2.347	2.343	
	— O1	1.657(14) × 2	1.641(11) × 2	Ti	— O4	1.879(10) × 2	1.866(9) × 2
	— O3	1.66(2)	1.623(16)	— O1	1.984(13) × 4	1.945(10) × 4	
Mean	1.651	1.632	Mean	1.949	1.919		

atomic distances are summarized in Table 6. The bond valences were calculated from the interatomic distances following the procedure of Brown and Altermatt (1985), using the parameters of Brese and O'Keeffe (1991). The values listed in Table 7 are weighted averages according to the occupancies in the final refinements. Owing to the

poor quality of X-ray diffraction data, the interatomic distances (Table 6) are not accurate enough for quantitative discussions. However, the bond valence sums are less far from the ideal values and are better than those estimated from data of the refinements with full occupancy F at the F3 site.

Table 7. Bond valence sums weighted on the occupancies for mieite-(Y)

Raw material									
	Y1 ($Y_{0.77}Dy_{0.23}$)		Y2 ($Y_{0.77}Nd_{0.23}$)		Ti ($Ti_{0.55}Al_{0.45}$)	Si	Sum		
O1			0.41	$\times 2 \downarrow$	0.52	$\times 4 \downarrow$	0.91	$\times 2 \downarrow$	1.84
O2	0.53		0.41				0.98		1.92
O3	0.50		0.47				0.91		1.88
O4			0.30	$\times 2 \rightarrow$	0.69	$\times 2 \downarrow \times 2 \rightarrow$			1.98
F1	0.40	$\times 2 \downarrow \times 2 \rightarrow$	0.34	$\times 2 \downarrow$					1.14
	0.32	$\times 2 \downarrow$							
F2	0.45	$\times 2 \rightarrow$							0.90
F3			0.26	$\times 2 \rightarrow$					0.52
($F_{0.55}$)									
Sum	2.92		2.94		3.46		3.71		
Annealed at 810 °C									
	Y1 ($Y_{0.77}Dy_{0.23}$)		Y2 ($Y_{0.77}Nd_{0.23}$)		Ti ($Ti_{0.55}Al_{0.45}$)	Si	Sum		
O1			0.42	$\times 2 \downarrow$	0.57	$\times 4 \downarrow$	0.96	$\times 2 \downarrow$	1.95
O2	0.59		0.46				1.00		2.05
O3	0.51		0.47				1.00		1.98
O4			0.33	$\times 2 \rightarrow$	0.71	$\times 2 \downarrow \times 2 \rightarrow$			2.08
F1	0.40	$\times 2 \downarrow \times 2 \rightarrow$	0.35	$\times 2 \downarrow$					1.15
	0.34	$\times 2 \downarrow$							
F2	0.49	$\times 2 \rightarrow$							0.98
F3			0.21	$\times 2 \rightarrow$					0.42
($F_{0.55}$)									
Sum	3.07		3.01		3.70		3.92		

DISCUSSION

The crystal structure of mieite-(Y) (Fig. 4) consists of infinite columns of corner-sharing TiO_6 octahedra decorated by SiO_4 tetrahedra, parallel to the c -axis. Although the linear chain was introduced as analogous to that in the crystal structure of brackebuschite [$Pb_2Mn^{3+}(VO_4)_2(OH)$] (Strunz and Nickel, 2001), the MnO_6 octahedra share their edges, in a different way from mieite-(Y) of corner-sharing, to form linear columns in the crystal structure of brackebuschite (Foley et al., 1997). The columns of corner-sharing TiO_6 octahedra in mieite-(Y) differs from the spiral-like chain composed of edge-sharing, strongly distorted TiO_6 octahedra in trimounsite-(Y) [$Y_2Ti_2SiO_9$] (Kolitsch, 2001), whereas these minerals are classified into a group 9.AG.25 (Strunz and Nickel, 2001). The coordination of TiO_6 shows mostly regular, but slightly flattened in the crystal structure of mieite-(Y). Two TiO_6 octahedra are linked with a SiO_4 tetrahedron bridging at 2 apices of the tetrahedron. The columns are linked by two independent Y polyhedra with different coordination, YO_2F_5 and YO_5F_3 . The combination of 7- and 8-coordinated Y sites in a crystal structure is the characteristic feature of mieite-(Y), and the same feature to magnesiorowlandite-(Y) (Matsubara et al., 2014). The 7-coordinated Y1 polyhedron (the mean Y1-O distance; 2.247 Å) is smaller than the 8-coordinated Y2 polyhe-

dron (the mean Y2-O distance; 2.343 Å) (Table 6). The larger Y2 site may be richer in larger light REEs such as Ce and Nd compared to the Y1 site. However, the occupancy parameters for Y1 and Y2 sites could not be refined independently owing to the poor quality of the X-ray diffraction intensity data (e.g., $R_{int.} = 0.1441$ and 0.1015). The relatively smaller equivalent displacement parameters (U_{eq}) of the larger 8-coordinated Y2 polyhedron, in comparison to the 7-coordinated Y1 polyhedron, suggests that the electron density is possibly higher, namely the occupation of lanthanoids (^{57}La - ^{71}Lu) is possibly greater inversely with ^{39}Y , at the Y2 site.

Although, the scattering factor for Dy was employed as the representative lanthanoids in the present crystal structure analysis, it is presumed that larger light REE, e.g., Nd, would be concentrated into the larger Y2 site, whereas smaller heavy REE, e.g., Dy, would occupy the smaller Y1 site together with Y. The prediction segregating REEs based on their ion sizes into the different sites, was speculatively applied for the bond valence sum (BVS) calculation as ($Y_{0.77}Dy_{0.23}$) and ($Y_{0.77}Nd_{0.23}$) for Y1 and Y2, respectively (Table 7), and resulted in BVS comparable to ideal values.

The chondrite-normalized lanthanoid distribution pattern of mieite-(Y) shows a trend rich in the heavy REEs (e.g., relatively high values of Lu and low values of La) in analogy with the pattern of magnesiorowland-

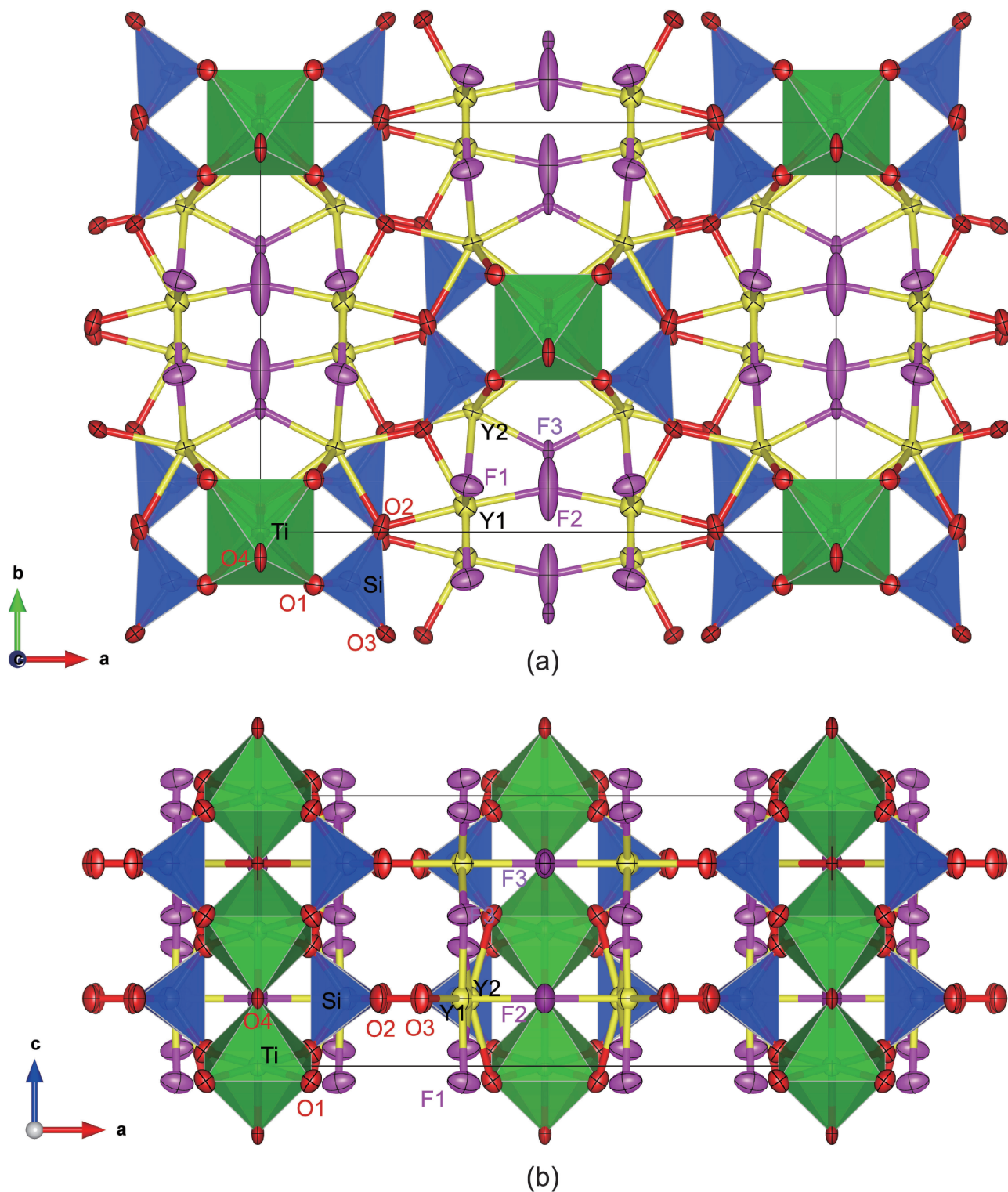


Figure 4. Projection views of the crystal structure of mieite-(Y) illustrated by VESTA (Momma and Izumi, 2011). Sites are indicated by colors as follows: green for Ti, blue for Si, yellow for Y, red for O, and purple for F. A projection onto (001) showing the *C*-centered configuration of columns of Ti-octahedra decorated by Si-tetrahedra and connected by Y-polyhedra (a). Another view onto (010) showing the columns of Ti-octahedra running parallel to the *c*-axis (b). The Ti-octahedra share their corners and are linked by the bridging Si-tetrahedra.

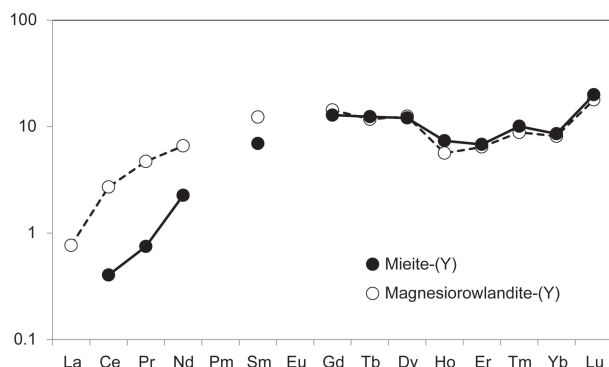


Figure 5. Chondrite-normalized lanthanoid distribution patterns of mieite-(Y) and magnesianrowlandite-(Y) (Matsubara et al., 2014).

ite-(Y) (Fig. 5). Values for exceedingly scarce lanthanoids whose concentration was under 0.01 wt%, the detection limit in the present electron microprobe analysis, such as Pm and Eu, are not plotted on Figure 5. The enrichment of light REEs, such as Ce and Nd, is not so significant in mieite-(Y) in comparison to magnesianrowlandite-(Y) (Matsubara et al., 2014). Both of these two minerals consist of the two independent crystallographic Y sites with differences in size and coordination number. Whereas the coordination numbers of Y sites are the same, 7 and 8, in these minerals, the sizes of polyhedra are respectively larger in magnesianrowlandite-(Y) than mieite-(Y). These trends in the size of polyhedron must be related to the averaged ionic size of REEs.

The refinement of crystal structure of mieite-(Y) suggested a vacancy in the F site. The electron microprobe analysis showed much deficiency in F ($F_{3.83}$ on the basis of 7 cations and 9 oxygen atoms *pfu*). The OH^- anion, detected in the FT/IR spectrum, was introduced to substitute for the F^- in the F sites. However, the position(s) of hydrogen atoms of OH^- anions could not be determined on the present difference Fourier map.

In the chemical composition of mieite-(Y) (Table 1), the heterovalent substitution of Al^{3+} for Ti^{4+} is remarkable. The observed minor substitutions of ($\text{Th}^{4+}, \text{U}^{4+}, \text{Ce}^{4+}$) for REE^{3+} and P^{5+} for Si^{4+} are not enough to compensate the major substitution of Al^{3+} for Ti^{4+} . A coupled substitution of $\text{Ti}^{4+} + \text{F}^- = \text{Al}^{3+} + \square$ was suggested as a charge compensating mechanism in the crystal structure of mieite-(Y) with the vacancy at the F3 site. A hypothetical end member derived from the substitution of $\text{Ti}^{4+} + \text{F}^- = \text{Al}^{3+} + \square$ is $\text{Y}_4\text{Al}(\text{SiO}_4)_2\text{O}[\text{F},(\text{OH})]_5$. This formula is something similar to that of kuliokite-(Y), $\text{Y}_4\text{Al}(\text{SiO}_4)_2(\text{OH})_2\text{F}_5$, whereas the crystal structures are not isomorphous to each other. The AlO_6 are isolated octahedra without any direct connections, but are linked by a

SiO_4 tetrahedron in the crystal structure of kuliokite-(Y) (Sokolova et al., 1986).

Mieite-(Y) from Souri Valley is isostructural with the ‘yftisite’ from Kola Peninsula, for which Balko and Bakakin (1975) determined the crystal structure. Mieite-(Y) can be classified in the Strunz class 9.AG.25, nesosilicates with additional anions; cations in (mostly) $> [6]$ and $> [6]$ coordination, and Dana class 52.4.4.3 with insular SiO_4 groups and O, OH, F, and H_2O , replacing ‘yftisite’ in these classes.

ACKNOWLEDGMENTS

The authors are grateful for helpful suggestions from Professor Peter A. Williams, the Chairman of IMA-CNMNC, and the members of IMA-CNMNC. Supporting data for single crystal diffraction were measured on an automated 4-circle diffractometer using monochromatic synchrotron radiation at the Beam Line 10A, Photon Factory, High Energy Accelerator Research Organization (PF, KEK), Japan [Project #2013G091].

DEPOSITORY MATERIALS

Depository items (cif files and F_o-F_c tables) are available online from <http://doi.org/10.2465/jmps.150106>.

REFERENCES

- Balko, V.P. and Bakakin, V.V. (1975) The crystal structure of the natural yttrium and rare-earth fluorotitanosilicate, $(\text{Y,TR})_4(\text{F,OH})_6\text{TiO}[\text{SiO}_4]_2$, (yftisite). *Zhurnal Strukturnoi Khimii*, 16, 837-842 (in Russian).
- Breese, N.E. and O’Keeffe, M. (1991) Bond-valence parameters for solids. *Acta Crystallographica*, B, 47, 192-197.
- Brown, I.D. and Altermatt, D. (1985) Bond-valence parameters obtained from a systematic analysis of the Inorganic Crystal Structure Database. *Acta Crystallographica*, B, 41, 244-247.
- Fleischer, M. and Jambor, J. (1977) Yftisite, in *New mineral names*. *American Mineralogist*, 62, 396.
- Foley, J.A., Hughes, J.M. and Lange, D. (1997) The atomic arrangement of brackebuschite, redefined as $\text{Pb}_2(\text{Mn,Fe})(\text{VO}_4)_2(\text{OH})$, and comments on Mn octahedra. *Canadian Mineralogist*, 35, 1027-1033.
- Harayama, S., Miyamura, M., Yoshida, F., Mimura, K. and Kurimoto, C. (1989) Geology of the Gozaishoyama district. *Quadrangle Series*, scale 1:50,000, pp. 145, Geological Survey of Japan (in Japanese with English abstract).
- International Tables for Crystallography, Volume C (1992) Wilson, A.J.C. Ed. pp. 883, Kluwer Academic Publishers, Dordrecht.
- Kolitsch, U. (2001) The crystal structure of trimounsite-(Y), $(\text{Y,REE})_2\text{Ti}_2\text{SiO}_9$: an unusual TiO_6 -based titanate chain. *European Journal of Mineralogy*, 13, 761-768.
- Matsubara, S., Miyawaki, R., Yokoyama, K., Shigeoka, M., Momma, K. and Yamamoto, S. (2014) Magnesianrowlandite-(Y), $\text{Y}_4(\text{Mg,Fe})(\text{Si}_2\text{O}_7)_2\text{F}_2$, a new mineral in a pegmatite at Souri

- Valley, Komono, Mie Prefecture, central Japan. *Journal of Mineralogical and Petrological Sciences*, 109, 109-117.
- Momma, K. and Izumi, F. (2011) VESTA 3 for three-dimensional visualization of crystal, volumetric and morphology data. *Journal of Applied Crystallography*, 44, 1272-1276.
- Nakamuta, Y. (1999) Precise analysis of a very small mineral by an X-ray diffraction method. *Journal of the Mineralogical Society of Japan*, 28, 117-121 (in Japanese with English abstract).
- Nickel, E.H. and Mandarino, J.A. (1987) Procedures involving the IMA Commission on New Minerals and Mineral Names and guidelines on mineral nomenclature. *American Mineralogist*, 72, 1031-1042.
- Pletneva, N.I., Denison, A.P. and Elina, N.A. (1971) A new variety in the group of rare-earth fluosilicates. *Material Mineralogy Kol'sk Poluostrova*, 8, 176-179.
- Sheldrick, G.M. (2008) A short history of SHELX. *Acta Crystallographica, A*, 64, 112-122.
- Sokolova, E.V., Egorov-Tismenko, Yu. K., Voloshin, A.V. and Pakhomovsky, Ya. A. (1986) Crystal structure of the new Y-Al silicate kuliokite-(Y), $Y_4Al[SiO_4]_2(OH)_2F_5$. *Soviet Physics Doklady*, 31, 601-603.
- Strunz, H. and Nickel, E.H. (2001) *Strunz Mineralogical Tables. Chemical-Structural Mineral Classification System*, 9th edition. E. Schweizerbart'sche Verlagsbuchhandlung (Nägele u. Obermiller), pp. 870, Stuttgart, Germany, 554-555.
- Toraya, H. (1993) The determination of unit-cell parameters from Bragg reflection data using a standard reference material but without a calibration curve. *Journal of Applied Crystallography*, 26, 583-590.

Manuscript received January 6, 2015

Manuscript accepted March 19, 2015

Published online May 30, 2015

Manuscript handled by Akira Yoshiasa